Electronics for HARPO: Design, Development and Validation of Electronics for a High Performance Polarised-Gamma-Ray Detector

Yannick Geerebaert, Denis Bernard, Philippe Bruel, Mickaël Frotin, Berrie Giebels, Philippe Gros, Deirdre Horan, Marc Louzir, Patrick Poilleux, Igor Semeniouk, Shaobo Wang, David Attié, Denis Calvet, Paul Colas, Alain Delbart, Patrick Sizun, Diego Götz, Sho Amano, Satoshi Hashimoto, Takuya Kotaka, Yasuhito Minamiyama, Shuji Miyamoto, Akinori Takemoto, Masashi Yamaguchi, Schin Daté, Haruo Ohkuma

***Abstract*—We designed and built an experimental apparatus based on a time projection chamber, a novel scheme for high performance γ-ray astronomy and polarimetry in the $\gamma \rightarrow e^+e^-$ regime. This presentation focuses on the electronics aspect of the detector and, in particular, on the versatile dedicated trigger system that we have developed which allowed us to take data on beam with a high γ-conversion signal efficiency and a high rejection factor for single tracks and upstream conversion background events.**

Our scheme allows for the selective collection of γ conversions in a high-background-rate environment, such as that which is present in orbit, with a fine 3D imaging of the events and very low (in particular electronics) background, at a mild cost in terms of the number of electronics channels and therefore of electrical power consumption.

***Index Terms*—Data acquisition, Electron multipliers, Gamma-ray detection, Gas detectors, High energy physics instrumentation, Particle tracking, Trigger.**

I. Introduction

HARPO (Hermetic ARgon POlarimeter) is an R&D program to characterise the operation of a gaseous detector as a high-angular-resolution and high-sensitivity telescope and polarimeter for cosmic γ-rays in the energy range MeV – GeV. It is the first phase of an ambitious program of a space telescope, using a new detection technique for γ-ray astronomy, the time projection chamber (TPC). The present detector is aimed at ground-validation tests, but we have designed it taking into account the constraints of space operation. Indeed, γ-ray pair telescopes currently in orbit suffer from a lack of sensitivity in the lower part of the γ-ray energy spectrum due to the technology they use (Si detector / W converter combinations) and the inefficiency of the trigger to distinguish events from the background noise in this energy range.

HARPO is an electron tracker that produces very fine 3D images of γ-ray conversions to e^+e^- pairs. To meet the requirements of a space environment, this is done at a low cost in terms of power consumption and data flow and uses a trigger system able to record relevant events in the presence of a large number of background noise tracks.

The present paper details the design, the integration and the validation of the electronic components of the HARPO TPC, from the drift volume where conversion occurs to the data being recorded on a PC. The electron amplification system and the trigger were identified to be challenging and critical functions and are therefore presented in more detail. The multi-stage electron amplification system is based on an innovative combination of two techniques, MICROMEGAS (Micro MEsh GAseous Structure) [1], [2] and GEM (Gas Electron Multiplier) [3].

Furthermore, the trigger has real-time analysis capabilities. It is able to switch between multiple configurations while taking data so that it is possible to analyse its performance in real-time for each run of data taking.

Polarimetry is performed by the analysis of the angular properties of pair conversion events that are reconstructed in the TPC. It is therefore important that the technical constraints related to space operation do not affect the angular resolution of the TPC.

II. Time Projection Chamber

As shown in Fig. 1, HARPO tracks pair creation events which follow from the interaction of a γ photon with a nucleus of a gas atom from the active volume of the detector. The

Manuscript received May 30, 2016. This work was funded by the French National Research Agency (ANR-13-BS05-0002).

Y. Geerebaert, D. Bernard, P. Bruel, M. Frotin, B. Giebels, P. Gros, D. Horan, M. Louzir, P. Poilleux, I. Semeniouk and S. Wang are with Laboratoire Leprince-Ringuet (LLR), École Polytechnique, CNRS/IN2P3, Route de Saclay, 91128 Palaiseau Cedex, France (telephone: +33 (0)1 69 33 56 14, e-mail: yannick.geerebaert@polytechnique.fr).

D. Attié, D. Calvet, P. Colas, A. Delbart and P. Sizun are with Institut de Recherche sur les lois Fondamentales de L'Univers (Irfu), CEA Saclay, 91191 Gif sur Yvette Cedex, France.

D. Götz is with Institut de Recherche sur les lois Fondamentales de L'Univers (Irfu), CEA Saclay, 91191 Gif sur Yvette Cedex, France and with AIM, CEA/DSM-CNRS-Université Paris Diderot, France.

S. Amano, S. Hashimoto, T. Kotaka, Y. Minamiyama, S. Miyamoto, A. Takemoto and M. Yamaguchi are with Laboratory of Advanced Science and Technology for Industry (LASTI), University of Hyōgo, 3-1-2 Koto, Kamigori-cho, Ako-gun, Hyōgo 678-1205, Japan.

S. Daté and H. Ohkuma are with Japan Synchrotron Radiation Research Institute (JASRI), 1-1-1, Kouto, Sayo-cho, Sayo-gun, Hyōgo 679-5198 Japan.

978-1-5090-2014-0/16/$31.00

HARPO TPC uses an Ar:isobutane (95:5) gas mixture in the range from 1 bar to 5 bar [4].

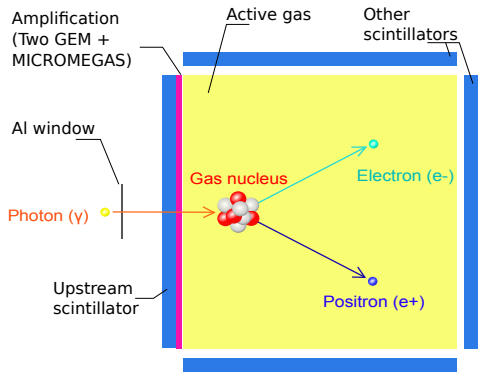

Fig. 1. Typical pair event created in the TPC gas.

The use of a TPC as an active target and γ photon telescope is unprecedented. The feasibility of such an instrument is based on a reduction, by several orders of magnitude, of the number of channels associated with a data rate reduction mechanism, at the price of sophisticated hardware and software, which enables the reconstruction of the initial event, while maintaining a good angular resolution.

A TPC achieves extremely fine imaging of the track(s) of an event. It can be likened to a 3D camera, for which the number of voxels is related to the size and resolution, and where the rate of shooting is the production rate of the events. The state of the art places the readout segmentation of a TPC between $n = 100$ and $n = 1000$ segments in each dimension x, y (transverse) and z (longitudinal). As the longitudinal dimension is given by the drift time, this represents, in the transverse direction, n^2, or 10^4 to 10^6 channels for a readout plane composed of pads. So, the total number of voxels to be stored in memory is proportional to n^3, which is considerable. Whereas, for a readout plane composed of strips, the number of channel and voxels are respectively proportional to $2n$ and $2n^2$. It should be emphasized that this reduction is only possible if the channel occupancy is low enough to avoid unsolvable ambiguities and comes at the cost of the need for off-line association of each x track to a track in the y view. For the HARPO TPC, the signal is collected by two orthogonal series of 288 strips (x, y), which, in our case, reduces the number of channels by a factor of 144 compared to the equivalent pixel sensor.

The tracking of events in a TPC involves many instrumental fields, such as gaseous radiation detectors (ionization, drift, amplification and collection), electronics (front-end, back-end and trigger), software (on-line operation, data quality monitoring, event reconstruction and analysis). Electronic equipment is needed in each of these instrumental fields.

III. Global Architecture of the Electronics

Fig. 2 shows a global view of the HARPO electronics, which can be divided into three parts:

- The electron drift and amplification spaces;
- The data acquisition (DAQ) of the amplified charges and;
- The trigger that rejects the huge background noise that comes mainly from the interaction of the beam with the material located upstream of the volume of gas.

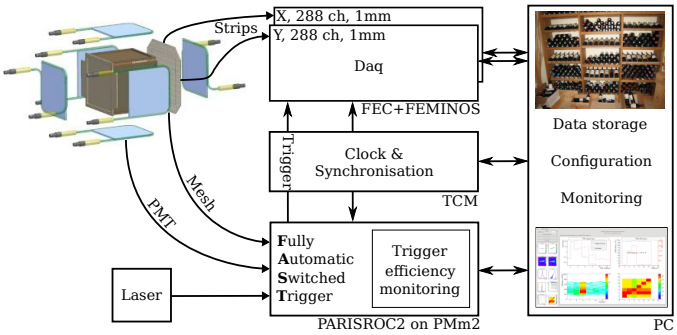

Fig. 2. A global view of the HARPO electronics. The TPC, surrounded by six scintillator plates, is on the left. It is readout by two modules that transfer their data to a PC and that are synchronised by a TCM. The trigger uses information from the beam (laser), the scintillators (via PMT) and the MICROMEGAS mesh.

A. Drift and Amplification

As shown in Fig. 3, the drift volume of the TPC is a 30 cm cubic field cage made from a simple 300 mm × 1200 mm, 160 µm-thick Kapton foil (Dupont Pyralux AP8545R) on which 60 Copper strips (3 mm wide, 35 µm-thick), with a pitch of 5 mm, are etched. The Kapton film is wrapped to form 60 rings, connected together with a pair of 10 MΩ resistors in parallel between each neighbouring ring. The cube thus formed is enclosed with a Copper cathode (made of a 1.6 mm-thick PCB covered with a plain 35 µm Copper layer) and a readout plane anode. This configuration imposes a uniform electric field in which electrons from ionization drift to the amplification system at a constant velocity $v_{\text{drift}} \approx 3.3\,\text{cm}/\mu\text{s}$.

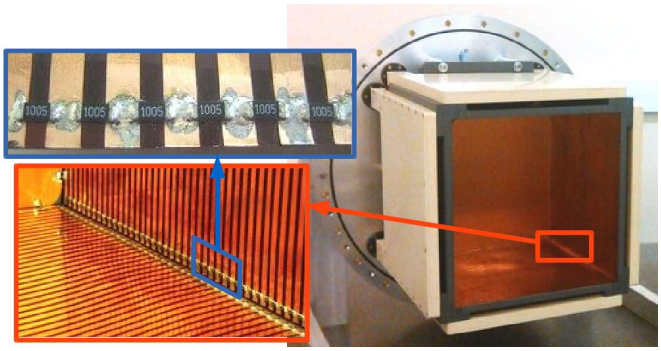

Fig. 3. Picture of the drift volume of the TPC with some details on the resistors.

The drifted electrons are amplified by a hybrid multi-stage amplification system composed of two GEM and one MICROMEGAS (128 µm-gap bulk).

Each GEM foil is a 406 mm × 406 mm, 50 µm-thick Kapton (Kaneka, APICAL NP) covered on each side by 5 µm of Copper. As shown in Fig. 4, the 300 mm × 300 mm active area is perforated by more than a million 70 µm-diameter holes at a pitch of 140 µm. When a high voltage is applied between the two faces, amplification takes place inside the

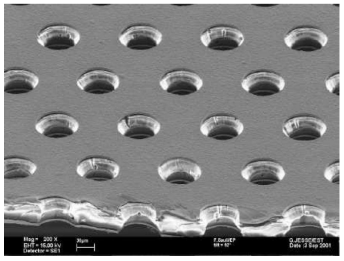

Fig. 4. Microscopic view of a GEM (Holes are 70 µm-diameter, with a pitch of 140 µm).

holes thanks to the high electric field. As a spark is often destructive for a GEM, the amplification gain is limited at a reasonably low value, here five for each GEM. Moreover, to limit the capacitance of the GEM and therefore the energy accumulated by its polarisation, the active surface is segmented on the top layer, into nine equal parts. Each GEM foil is glued on a 2 mm-thick polymer frame containing four very thin (400 µm) partition walls under the active area. Those spacers lead to a small local efficiency loss but are required to guarantee uniformity in the gaps between each layer. Small notches are present in the spacers and on the edges of the frames to ensure proper gas flow during filling or emptying.

As shown in Fig. 5, two of these framed-GEM are placed above the MICROMEGAS.

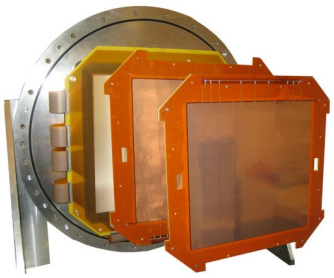

Fig. 5. Photo-montage of stepped electron amplification system formed by two GEM and one MICROMEGAS.

The MICROMEGAS is a 406 mm × 406 mm, 3 mm-thick standard FR4 PCB, with three Copper layers, on top of which a fine stainless steel woven mesh (18 µm wires at a pitch of 63 µm, BOPP SD 45/18) is held at a gap distance of 128 µm from the collection plane by polyimide (Dupont Pyralux PC1025) pillars, 400 µm in diameter, at a pitch of 2.5 mm.

The active area of 288 mm × 288 mm is formed by two sets of 288 crossed strips at a pitch of 1 mm (Fig. 6). In the x direction, the strips are simple Copper traces, whereas in the y direction they are formed by pads connected together by an internal layer. When the mesh is set to a high voltage (−420 V typically at 2 bar) with respect to the collection plane, amplification takes place in the gap.

The combined amplification of both the GEM and the MICROMEGAS (5×5×100) provides a wide dynamical range of operation while limiting the risk of destructive sparks in either the GEM or in the MICROMEGAS, especially at high pressure where the bias voltages are higher. The GEM and

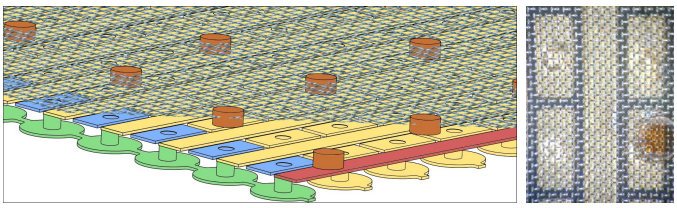

Fig. 6. Left: Layout of the MICROMEGAS. For the PCB-based plane, only the Copper is shown. One x strip is coloured in red and one y pseudo-strip is in blue. The y pseudo-strips are segmented in pads, connected together via an internal layer (green). The mesh (whose corner is cut) is held up at 128 µm out of the readout plane, by pillars with diameter of 400 µm, at a pitch of 2.5 mm. Right: Picture showing a detail of the MICROMEGAS.

MICROMEGAS combinations have been characterised with a ^{55}Fe source at 1 bar and commissioned with cosmic rays in the range from 1 bar to 2 bar [5].

A layout of the field cage resistor voltage divider is shown in Fig. 7.

The resistors have been measured, sorted and coupled to achieve a uniformity of the ohmic value of the pair to better than 10^{-4}. The primary reason, however to avoid a single-resistor chain is that in the case of the breaking of a solder joint of one of the resistors, the total high-voltage of the full chain (several kV) would be applied over a few millimeters, which would lead to sparking and possibly to breakdown. For the same reason, the last ring of the field cage (nearest to the amplification system) is connected through a 10 MΩ security resistor to the ground in case of a disconnection of the V_r power supply.

Table I summarizes the numerical values of polarisation voltages and electric fields of the TPC for typical operating conditions at 2 bar.

TABLE I
POLARISATION VOLTAGES AND ELECTRIC FIELDS IN TYPICAL OPERATING CONDITIONS AT 2 bar.

TPC region	Name	Voltage (V)	Field (kV/cm)	ΔV (V)	Distance
Drift	V_k	-8046			
	V_r	-1446	0.22	6600	30 cm
Drift-GEM gap			0.22	66	3 mm
Top GEM	V_{tt}	-1380			
amplification	V_{tb}	-1060	64.00	320	50 µm
Top transfer			0.80	160	2 mm
Bottom GEM	V_{bt}	-900			
amplification	V_{bb}	-580	64.00	320	50 µm
Bottom transfer			0.80	160	2 mm
MICROMEGAS	V_{mesh}	-420			
Readout plane		0	32.81	420	128 µm

B. Data Acquisition

The 576 charges collected by the x and y strips are extracted from the pressure vessel via two signal PCB feedthroughs that are glued into an opening in the flanges. After the PCB is positioned through the flange aperture with a nitrile 70sh-pb701 O-ring, fixing is performed with a standard Araldite glue.

Outside the pressure vessel, two 288-channel Front-End Cards [6] (FEC, Fig. 8a) are connected to the signal

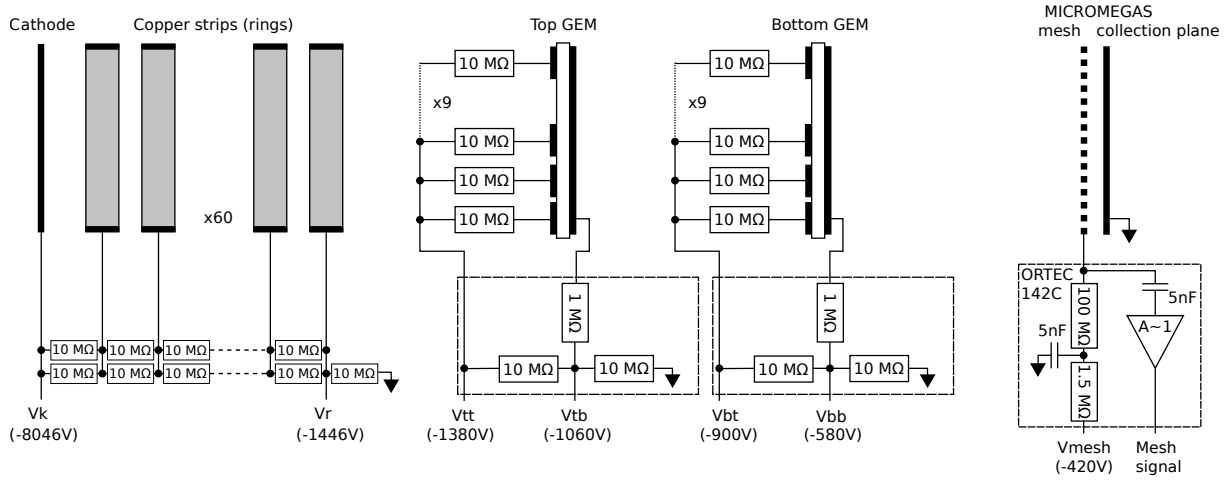

Fig. 7. View of the TPC voltages. From left to right: Resistor divider used to set a uniform electric field in the drift part of the TPC (between cathode and the top layer of top GEM). Two GEM with their nine sectors and protection resistors (holes in GEM do not appear on this drawing). The voltage applied to the mesh of the MICROMEGAS pass trough a filter included inside an ORTEC pre-amplifier 142C. The voltages indicated are typical values in nominal operating conditions.

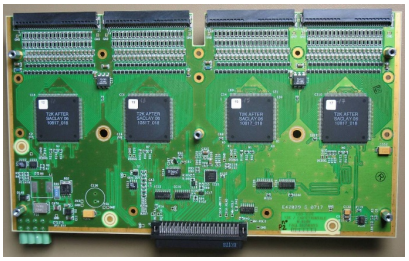

(a) FEC equiped with four AFTER chips.

(b) FEMINOS.

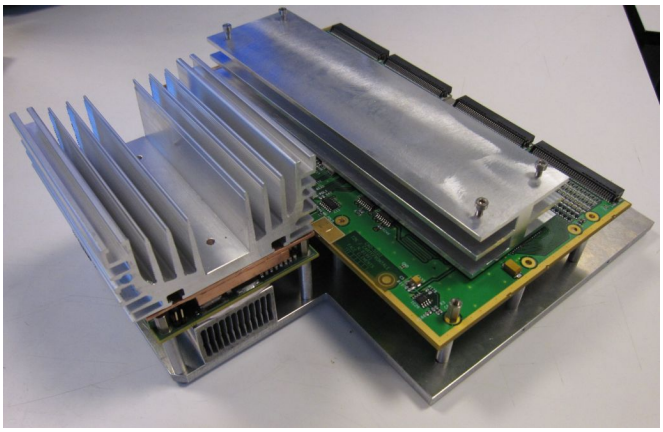

(c) One HARPO fanless DAQ module composed of one FEMINOS and one FEC equipped with four AFTER chips.

Fig. 8. Pictures of the DAQ hardware. HARPO uses two of these (x, y).

feedthroughs. Each FEC contains four AFTER [7] (ASIC For TPC Electronic Readout) chips and an external 12-bit quad-channel ADC (Analog Devices AD9229). This ASIC was specifically designed for TPC applications. It consists of 72 multiplexed channels including a charge sensitive amplifier (four input ranges from 120 fC to 600 fC), a filter stage and a Switch Capacitor Array (SCA) of 511 cells used as analog memory. While taking data, the incoming charges are continuously stored in the SCA circular buffer at a sampling frequency of 33 MHz until a trigger occurs. The frequency of the SCA write clock is obtained by dividing the 100 MHz reference clock by an integer factor (m) that can be chosen from 1 to 63. For $m = 3$ (or 30 ns sampling period), at the velocity of 3.3 cm/µs, the electrons cover a distance of 1 mm in 30 ns, so the z longitudinal binning is 1 mm, that is, the same as the transverse (x, y) binning. The whole drift volume of 300 mm is then contained in 300 cells of the SCA.

Each FEC is controlled by a FEMINOS board [8] (Fig. 8b). It is based on a commercial off-the-shelf (COTS) module (Enclustra, Mars MX2) so as to have a short development time and low cost. The dedicated FPGA firmware together with the C-coded shell (without OS) on a MicroBlaze soft processor in fast enough for the control of the four front-end chips enabling them to drain the full bandwidth of a FEC board and therefore to achieve the theoretical minimum dead time ($\sim$ 1.6 ms) of the AFTER chip. In other words, the absolute maximum acquisition rate of an AFTER chip is $\sim$ 600 Hz. Both FEMINOS boards have a Gigabit Ethernet link and are connected to the acquisition PC through a switch.

A raw event represents 335 kBytes of data, but thanks to the low channel occupancy, most of the data are zero-suppressed in the FPGA and then a mean of 3.3 kBytes per event are transmitted to the PC where they are stored for on-line monitoring and off-line physics analysis.

As shown in Fig. 2, the 100 MHz reference clock, the trigger and some control signals are delivered to both FEMINOS by one TCM (Trigger and Clock Module, Fig. 9) which is based on the same COTS as the FEMINOS.

These versatile boards (FEC, FEMINOS and TCM), as well as the AFTER chip were originally designed at IRFU for the T2K and MINOS experiments. Details on the main characteristics and performance studies can be found in [7], [6], [9], [8].

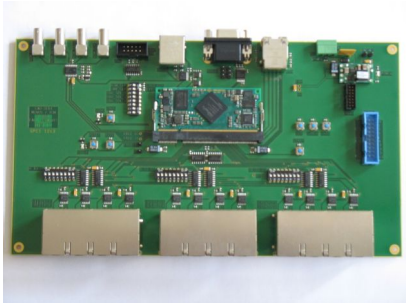

Fig. 9. Picture of the Trigger and Clock Module (TCM), using a Mars MX2 module from Enclustra.

C. Trigger

Separate trigger schemes were developed for cosmic-ray tests in the laboratory and for data taking on a γ-ray beam. The cosmic-ray trigger uses a simple coincidence between scintillator signals. For the in-beam operation, a much more sophisticated system was designed.

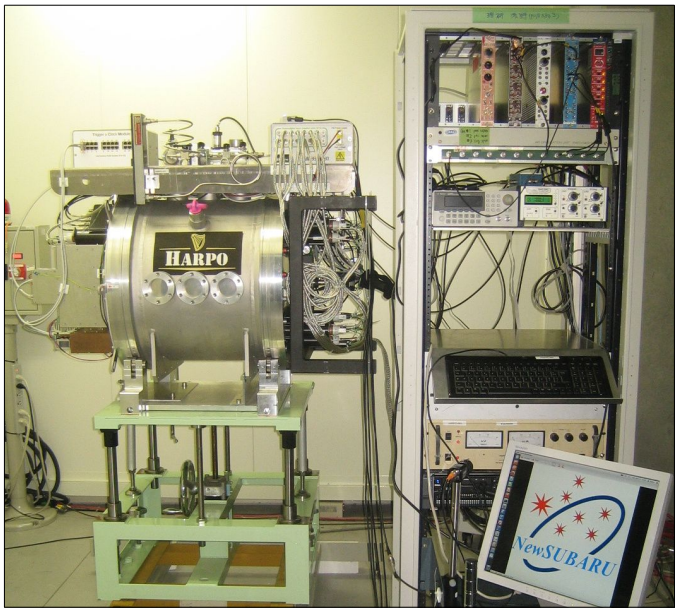

Fig. 10. Picture of HARPO exposed to a polarised γ-ray beam in 2014 at NewSUBARU, Japan. The detector is positioned so that the photon beam is aligned with the drift direction, z, of the TPC, entering through the readout side, and exiting through the cathode.

As shown in Fig. 10, the HARPO TPC was set up in the NewSUBARU (Hyōgo, Japan) polarised photon beam line [10]. Fig. 11 shows the architecture of the photon beam. It is produced by the Inverse Compton Scattering (ICS) of an optical laser on a high energy (0.6 GeV to 1.5 GeV) electron beam. Using lasers of various wavelengths and different beam energies [11], we scanned 13 photon energies from 1.74 MeV to 74 MeV.

The probability of conversion is directly correlated with the density of the material traversed. The matter placed between the TPC gas and the γ-ray beam has to be as thin as possible. Starting from the γ-ray source, we have:

- a 0.5 mm-thick aluminium window,

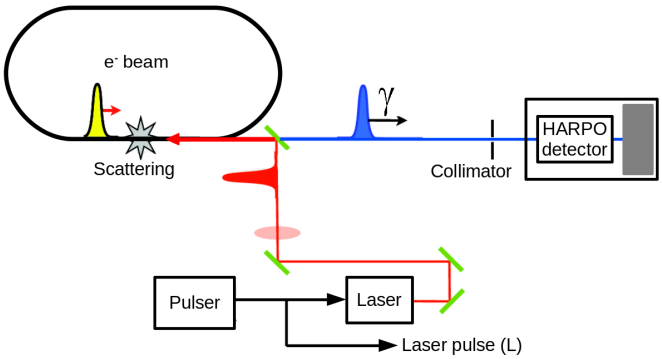

Fig. 11. Architecture of the NewSUBARU polarised photon beam line. γ beam is produced by the Inverse Compton Scattering (ICS) of an optical laser on a high energy electron beam.

- the upstream scintillator enclosed inside a PVC box and coated with a reflective sheet
- the multi-staged electron amplification composed of:
  - two GEM layers, $\approx 60\,\mu$m each
  - one MICROMEGAS, which is a few-μm-thick metallic mesh held above a 3 mm-thick PCB.

So the major part of the background comes from the interaction of the beam with the upstream material. In the presence of this noise, the dead time induced by the readout of the AFTER chips (1.6 ms) requires us to select the interesting events before their digitization.

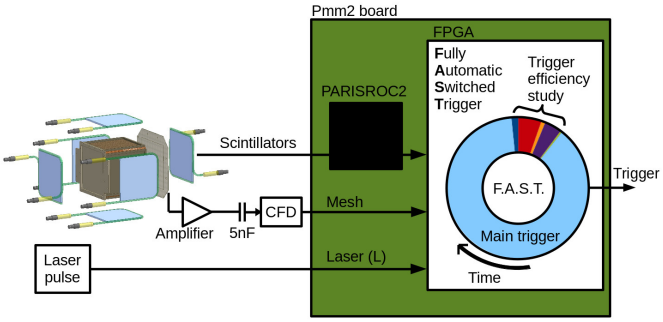

Fig. 12. Global architecture of the trigger.

For this purpose, we developed a sophisticated trigger which combines the signals from the scintillators, from the mesh of the MICROMEGAS and from the laser. The trigger system includes several "trigger lines" that allow the impact of each of the above ingredients (scintillator, mesh, laser) to be isolated and studied for signal and for background events.

The general architecture of the trigger is shown in Fig. 12. The trigger working scheme can be understood by taking into account the following three time scales:

1) A γ-ray creates a pair in the gas, the e^+ and e^- ionize the gas along their path, they cross a scintillator where a light pulse is generated (a few nanoseconds),
2) Under the effect of the electric field, free electrons drift towards the amplification plane and induce a signal on the mesh (up to ten microseconds),

3) Upon a trigger, the writing in analog memories of the AFTER chips stops and the charges contained in all of time buckets of all channels are digitized in series (a few milliseconds).

Fig. 13 shows the data of a typical event in one axis (here x) and a timing diagram of the involved signals within the two first time scales.

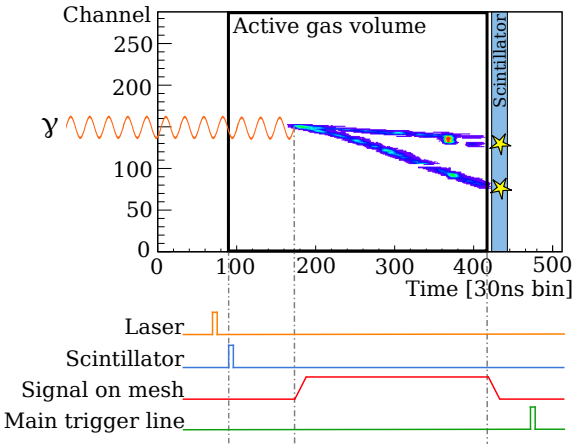

Fig. 13. Typical timing of trigger in TPC.

Each scintillator is equipped with a pair of photomultiplier tubes (PMTs) which are read out by a PARISROC2 chip [12] mounted on a PMm2 board. This board was previously designed for a R&D project for the next generation of proton decay and post-SuperKamiokande neutrino experiments [13]. This board records the charge of each PMT thanks to the auto-trigger capability of the PARISROC2 chip. We use this feature as a trigger efficiency monitor. Fig. 14 shows a picture of the PMm2 board and Fig. 15 shows a picture of the final PMT configuration. On top, PMm2 is inside its box, connected to the PMTs via shielded cables.

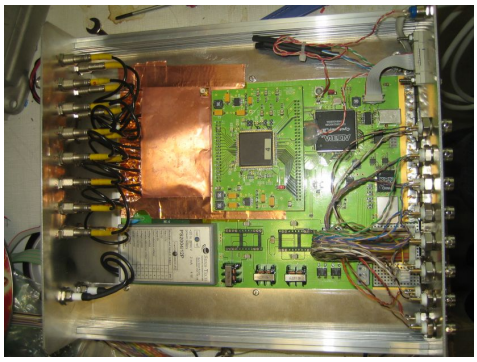

Fig. 14. Picture of the PMm2 board with a PARISROC2 chip and a FPGA.

A veto on the upstream scintillator rejects most of the tracks that come with the beam. γ conversions that take place in the PCB, downstream of the scintillator, are rejected by an additional veto based on the presence of a very early signal in the mesh of the MICROMEGAS.

The signal from the mesh, which is long (up to $10\,\mu s$) with an unpredictable shape, corresponds to the time (that is z) distribution of the tracks in the TPC. To improve the trigger timing and make it independent from the magnitude of the mesh signal, we use a constant-fraction discriminator (CFD), which shows the beginning of the signal, and therefore the longitudinal position of the beginning of the track. By using either the scintillators or the laser signal, we can measure the delay between the start of the event and this signal to build a veto on tracks created upstream or very early in the TPC ($< 1\,\mu s$).

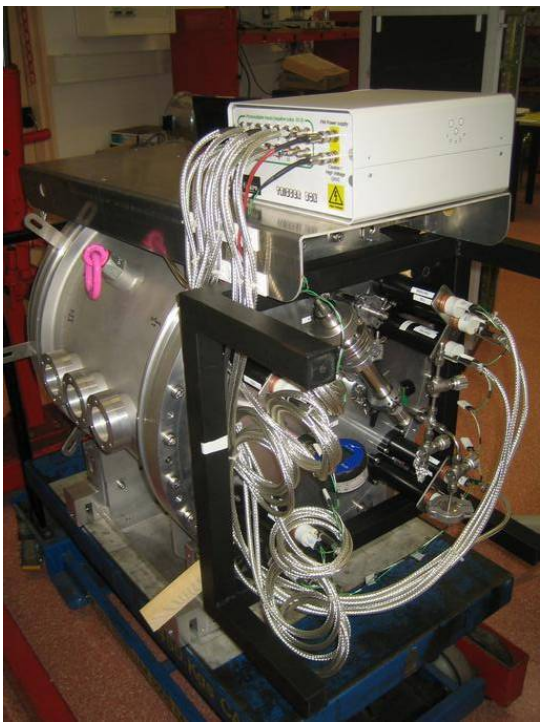

Fig. 15. Picture of the final PMT configuration. On top, PMm2 is inside its box, connected to the PMTs via shielded cables. The unique high voltage PMT power supply can be remotely adjusted.

We have used the laser signal from the beam, whenever available (i.e. pulsed lasers), in coincidence with HARPO's internal trigger.

In addition to the original firmware of the PMm2 FPGA, we developed a trigger function, called FAST (for Fully Automatic Switched Trigger), built from the discriminated signals of the PMTs, of the laser and of the MICROMEGAS mesh. Thirteen trigger lines were defined, each with different combinations of the signals so as to enable us to study their efficiency and background rejection capabilities.

The main trigger line selects pair-creation events in the TPC gas. It is composed of:

- a veto on the upstream scintillator,
- a signal on the mesh of the MICROMEGAS with a veto based on the presence of a very early signal,
- a signal in at least one of the five other scintillators,
- a laser signal, whenever available (i.e. the pulsed laser), in coincidence with the signal in the scintillators.

While taking data, FAST switches periodically between each trigger line, for a duration that is allocated depending upon the configuration. The duration of each line is configurable from $0\,\mathrm{ms}$ to $65535\,\mathrm{ms}$ in steps of $1\,\mathrm{ms}$.

In typical beam operation, 9 s are allocated to the main trigger line and 1 s is shared between five trigger lines dedicated to the efficiency study.

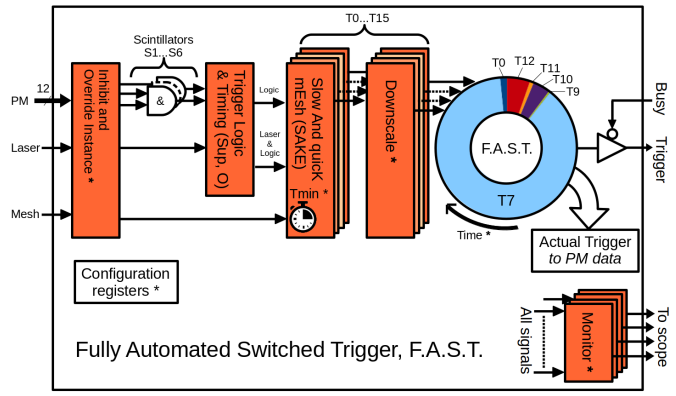

Fig. 16. Functional diagram of the fully automated switched trigger, implemented in the firmware of the PMm2's FPGA.

The FAST functional diagram, implemented in the FPGA, is shown in Fig. 16. The signal path goes from left to right: In the case of a problem, each signal that participated in the trigger can be disabled and set to logic level "0" or "1" by Inhibit and Override Instance (IOI). Then, the PMTs signals are paired with six AND logic gates to form scintillator signals, which are then combined with the laser pulse signal in Trigger Logic and Timing (TLT). TLT generates, in a time window, the logical combinations of those six scintillator signals and of the laser pulse needed by each trigger line. Each triggered module Slow And quicK mEsh (SAKE) is sensitive to the rising edge of the mesh signal within the drift time. In the case of a trigger period lower than the dead time of the DAQ, the related trigger line can be downscaled. Finally, FAST delivers the selected trigger signal to the DAQ only when the latter is not busy.

In parallel and in real time, FAST adds the identification of the current trigger to the PMT data that are sent to the PC. Furthermore, the timestamps of FEMINOS and PMm2 are synchronised at the beginning of each run by the TCM. This allows the on-line monitoring software to associate the TPC data (from both FEMINOS) with PMT data.

IV. Software

The HARPO software, which operates under a Linux Ubuntu operating system (OS), is heterogeneous.

For the DAQ:

- The run control is performed with a shell script.
- The control and the readout of the two FEMINOS and the TCM is carried out by three independent Linux processes, each running a command-line client.
- Another simple command-line client controlling and reading out the PMm2 trigger data.
- An on-line monitoring software, based on the CERN root/C++ analysis framework, synchronises and combines the data from the two FEMINOS and the PMm2. A fraction of the events (typically 1 in 10) is analysed to provide real time information about the state of the detector and the quality of the data such as the trigger rate, the occupancy and to provide a basic event categorisation, as shown in Fig. 17.

An off-line analysis software, also based on the CERN root/C++ analysis framework, performs the full reconstruction of the data. Finally, the physics simulations are performed within GEANT4/C++ framework.

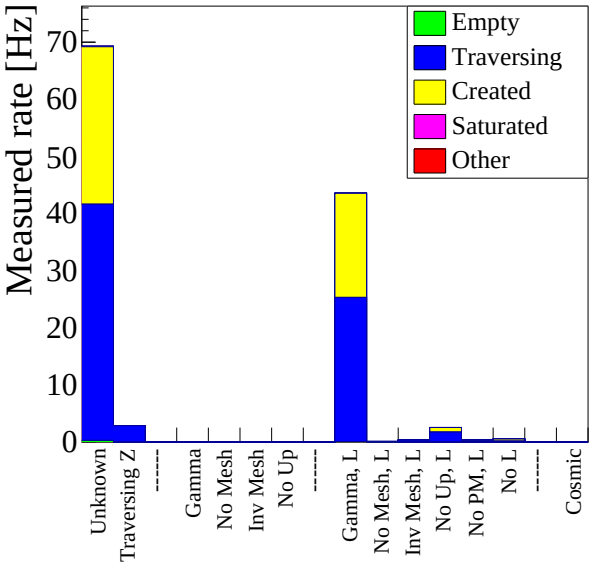

Fig. 17. View of the trigger rate, processed by the on-line monitoring software, for each active line for a typical run. Colours represents the event categorisation.

In addition, some equipment (power supplies, temperature and pressure gauges,..) is controlled by the software provided by the manufacturer, using a Windows OS virtual machine.

For each run, the beam and detector parameter information is stored in a database based on phpMyAdmin.

The documentation is stored on a subversion (svn) server and the analysis software is managed with a Git repository.

V. TPC Operation and Performance

Before operating the detector in beam, we characterised the TPC in our laboratory with comics rays [14].

For the in-beam operation, the detector was positioned so that the photon beam was aligned with the drift direction, z, of the TPC, entering through the readout side, and exiting through the cathode. The analysis software allowed us to align the detector with the beam.

60×10^6 events were recorded at 13 energy points with a polarisation of either $0\,\%$ or $100\,\%$. In addition, for each energy and beam-polarisation configuration, data was taken with the TPC rotated by four values $(-45, 0, +45, +90\,^\circ)$ of the "azimutal" angle, around the beam axis, so that the systematic bias of the polarisation measurement, induced by the strong non-cylindrical-symetric (cubic, actually) structure of the detector, can be studied and corrected. Furthermore, to assess the absence of any residual experiment bias, data with random γ-beam polarisation, that is a zero linear polarisation fraction, was taken.

Otherwise, we found, especially at high beam energy, that the charge sensitive amplifiers (SCA) of the AFTER chips

were often saturated. Indeed, the recovery time of the CSA (few µs) is slightly longer than the write period (30 ns) of the data. Therefore, after a huge charge deposit on a strip, the related channel becomes blind until the CSA recovers. This effect also appears when an accumulation of small individual charges arrive at a channel during the drift time. This problem was greatly amplified by the beam configuration, which accumulated the signal on a few channels.

This problem was reduced by changing the detector alignment, which spreads the signal out over several channels. But, even trough this effect was considerably minimized, it still affected a large fraction of the beam data. This problem does not affect cosmic data that have random directions and a lower rate.

The trigger is effective rejecting $99.2\,\%$ of the noise. This means that this trigger suppresses the huge background rate from the accelerator and from the upstream conversions (up to 5 kHz) by a rejection factor greater than two orders of magnitude.

The data rate acquired by the main trigger line varies depending on the power and energy of the beam. The γ conversion rate in the gas is about 50 Hz on average for the data taking, which is compatible with the predicted rate. Pair creation events represent $51\,\%$ of the recorded data.

VI. Conclusions

The electronics for HARPO, which is an electron tracker that produces very fine 3D images of γ-ray conversions to e^+e^- pairs, has been presented. With the HARPO TPC we have been able to collect about 60×10^6 events, comprising an estimated 30×10^6 γ conversion events during an experimental campaign on a γ-ray beam at an average signal rate of 50 Hz, despite the incoming background rate being in the 10 kHz range. This would not have been possible without the sophisticated trigger system that allowed us to select γ conversions in the gas with an efficiency larger than $50\,\%$ with a background rejection factor of more than two orders of magnitude. The monitoring of each component of the trigger system by the analysis of specific trigger lines was instrumental in achieving this performance. The high-quality data that we have collected in the γ energy range 1.7 MeV to 74 MeV are being analysed: preliminary results show images with a very low level of background that enable tracking with excellent precision.

HARPO demonstrates that the design of a space TPC is viable. The next step will be the design of a balloon-borne TPC, in particular of its trigger, which is a key ingredient for a successful space telescope.

Acknowledgment

We wish to thank L. Ropelewski *et al.* from the RD51 laboratory at CERN for their efficient support in the manufacture of the framed-GEM.

References

[1] I. Giomataris, R. De Oliveira, S. Andriamonje, S. Aune, G. Charpak, P. Colas, A. Giganon, P. Rebourgeard, and P. Salin, "Micromegas in a bulk," *Nucl. Instrum. Meth.*, vol. A560, pp. 405–408, 2006.

[2] Y. Giomataris, P. Rebourgeard, J. P. Robert, and G. Charpak, "MICROMEGAS: A High granularity position sensitive gaseous detector for high particle flux environments," *Nucl. Instrum. Meth.*, vol. A376, pp. 29–35, 1996.

[3] F. Sauli, "GEM: A new concept for electron amplification in gas detectors," *Nucl. Instrum. Meth.*, vol. A386, pp. 531–534, 1997.

[4] D. Bernard, "HARPO - A gaseous TPC for high angular resolution γ-ray astronomy and polarimetry from the MeV to the TeV," *Nucl. Instrum. Meth. A*, vol. 718, pp. 395–399, 2013.

[5] P. Gros *et al.*, "HARPO - TPC for High Energy Astrophysics and Polarimetry from the MeV to the GeV," *Proceedings of Science*, vol. TIPP2014, p. 133, 2014.

[6] P. Baron, D. Besin, D. Calvet, C. Coquelet, X. De La Broise, E. Delagnes, F. Druillole, A. Le Coguie, E. Monmarthe, and E. Zonca, "Architecture and implementation of the front-end electronics of the time projection chambers in the T2K experiment," *IEEE Trans. Nucl. Sci.*, vol. 57, pp. 406–411, 2010.

[7] P. Baron, D. Calvet, E. Delagnes, X. De La Broise, A. Delbart, F. Druillole, E. Mazzucato, E. Monmarthe, F. Pierre, and M. Zito, "After, an ASIC for the readout of the large t2K time projection chambers," *IEEE Trans. Nucl. Sci.*, vol. 55, no. 3, pp. 1744–1752, 2008. [Online]. Available: http://ieeexplore.ieee.org/stamp/stamp.jsp?arnumber=4545069

[8] D. Calvet, "A Versatile Readout System for Small to Medium Scale Gaseous and Silicon Detectors," *IEEE Trans. Nucl. Sci.*, vol. 61, no. 1, pp. 675–682, 2014.

[9] D. Calvet, I. Mandjavidze, B. Andrieu, O. Le Dortz, D. Terront, A. Vallereau, C. Gutjahr, K. Mizouchi, C. Ohlmann, and F. Sanchez, "The back-end electronics of the time projection chambers in the T2K experiment," *IEEE Trans. Nucl. Sci.*, vol. 58, pp. 1465–1471, 2011.

[10] K. Horikawa, S. Miyamoto, S. Amano, and T. Mochizuki, "Measurements for the energy and flux of laser compton scattering -ray photons generated in an electron storage ring: Newsubaru," *Nucl. Instrum. Meth.*, vol. 618, no. 1-3, pp. 209 – 215, 2010. [Online]. Available: http://www.sciencedirect.com/science/article/pii/S0168900210005449

[11] A. Delbart *et al.*, "HARPO, TPC as a gamma telescope and polarimeter: First measurement in a polarised photon beam between 1.7 and 74 MeV," *Proceedings of Science*, vol. ICRC2015, p. 1016, 2015.

[12] S. Conforti Di Lorenzo *et al.*, "PARISROC, an autonomous front-end ASIC for triggerless acquisition in next generation neutrino experiments," *Nucl. Instrum. Meth.*, vol. A695, pp. 373–378, 2012.

[13] B. Genolini *et al.*, "PMm2: Large photomultipliers and innovative electronics for the next-generation neutrino experiments," *Nucl. Instrum. Meth.*, vol. A610, pp. 249–252, 2009.

[14] D. Bernard *et al.*, "HARPO: a TPC as a gamma-ray telescope and polarimeter," *Proc. SPIE Int. Soc. Opt. Eng.*, vol. 9144, p. 91441M, 2014.